European Journal of Orthodontics 32 (2010) 354–362
doi:10.1093/ejo/cjp147
Advance Access Publication 15 January 2010

© The Author 2010. Published by Oxford University Press on behalf of the European Orthodontic Society.
All rights reserved. For permissions, please email: journals.permissions@oxfordjournals.org

Natural reference structures in the human mandible: a systematic search in children with tantalum implants

S. D. Springate
Eastman Dental Institute, London, UK

SUMMARY The purpose of this study was to locate stable natural reference structures (NRS) in the mandible as seen on lateral cephalometric radiographs. The material consisted of pairs of serial radiographs of 34 children (15 males and 19 females aged 8.7–14.3 years at the initial radiograph, with a mean interval of 4.1 years between radiographs). Each child had three Björk type tantalum implant markers in the left side of the mandible. The pairs of radiographs were converted to digital image format, superimposed, and registered using stable implants. Potential NRS were located by visual examination of the superimposed images. The morphological and spatial stability of these potential NRS were tested using automated computer–based analysis employing cross-correlation.

NRS were located in each subject (range 4–15 NRS). The number of NRS was statistically significantly correlated with age at the initial radiograph (r_{rank} = 0.39, P = 0.02) but not with the interval between the radiographs (r_{rank} = 0.21, P = 0.23). Two groups of NRS were found: a small group of amorphous bony condensations and prominent trabeculae mainly in the body and ascending ramus, and a larger group of nine anatomical structures consisting of neurovascular canals and bony striae close to the endocortical surface of the inferior cortex. Two bony structures previously reported as stable (the inner inferior contour of the symphysis and prominent trabeculae within the symphysis) were generally found to drift, presumably because of gradual differential remodelling, making them unreliable as NRS. Based on these findings, two alternative methods are proposed for accurate mandibular superimposition.

Introduction

The earliest cephalometric studies used the inferior border of the mandible, and later the mandibular plane, as the reference sites for the evaluation of growth and treatment changes in the mandible and mandibular dentition. By the late 1940s, however, the findings from vital staining studies in growing primates began to cast doubt on the validity of this procedure (Brodie, 1949). These doubts were later confirmed in human subjects by the classic implant studies of Björk (1955, 1963), which showed that the inferior border and angle of the mandible undergo extensive differential remodelling during growth.

As a result of these studies, it has been suggested that using the mandibular plane or inferior border of the mandible as the site of superimposition will lead to incorrect representation of the changes taking place in the mandible and mandibular dentition (Björk, 1969; Mathews and Payne, 1980; Isaacson *et al.*, 1981; Björk and Skieller, 1983).

While it is now widely accepted that stable implanted markers offer the most valid means of superimposing cephalometric tracings, such markers are seldom available. In addition, the insertion of implanted markers is generally considered unethical for routine cephalometric evaluation.

As a result of his investigations in subjects with metallic implants, Björk (1963, 1969) suggested four anatomical structures, which might usefully act as natural substitutes for implants in the mandible. Later, a fifth structure was added to the list by Björk and Skieller (1983). The exact methods by which these structures were detected and their stability verified, however, have not been published, although Björk (1963) implied that their detection was not the result of intentional or systematic analysis.

Although the short-term stability of Björk's original structures has been corroborated by the independent implant study of Julius (1972), other researchers have questioned their usefulness because of the difficulty in locating, tracing, and superimposing them, especially where bilateral images occur (Feasby, 1981; Cook and Gravely, 1988; Isaacson, 1996). This difficulty inevitably leads to high levels of imprecision regardless of the validity of the structures. This imprecision can be improved by replication and averaging but there is some evidence that similar mean positions may not be achieved by Björk's structures and implants (Springate and Jones, 1998).

The purpose of this study was to locate stable anatomical structures on mandibular lateral cephalometric images that could be reliably used for mandibular superimposition. It was hoped that systematic analysis of serial cephalometric radiographs of subjects with stable tantalum implants might reveal additional natural reference structures (NRS) that could be used to supplement, or substitute for, Björk's reference structures where they were either not present or not easily identifiable.

Materials and methods

The material for this investigation consisted of pairs of serial lateral cephalometric radiographs of children drawn from the implant research files of the Department of Orthodontics of the University of Washington, Seattle and from the Mathews' implant files of the University of California at San Francisco. Each subject had three Björk type tantalum marker pins (Björk, 1968) implanted unilaterally in the left side of the mandible.

No subjects with known mandibular or craniofacial pathology were included in the study. Pairs of serial radiographs were selected from the available material on the basis of image quality and the similarity of the mandibular projection in both radiographs of each subject.

The radiographs of 34 subjects (15 males and 19 females) fulfilling these criteria were available for study. The subjects ranged in age from 8.7 to 14.3 years at the initial radiograph, with a mean interval of 4.1 years (standard deviation = 1.25 years) between the radiographs. Although not deliberately selected, the sample included the full range of antero-posterior skeletal discrepancies (skeletal Class I, Class II, and Class III) and high and low mandibular angles, and included both treated (extraction and non-extraction) and untreated cases.

Experimental method

The experimental method consisted of two stages: (1) the visual identification of 'candidate sites'—potentially stable sites which appeared in both the earlier and later radiographs—and (2) the subsequent testing of the morphological and spatial stability of the candidate sites using automated computer–based analysis of the images.

For ease of manipulation, the radiographs were first converted into a digital format using a flatbed scanner (DuoScan HiD, Agfa-Gevaert, Mortsel, Belgium) and the comparisons and measurements carried out by computer. The radiographs were scanned to give a pixel size of 0.08 × 0.08 mm. The images of each pair of radiographs were then adjusted to similar contrast and brightness levels.

Validation of implant stability

It is known that implants may be displaced by periosteal drag resulting from inadequate depth of placement, from electrolytic action, and by uncovering during periods of rapid remodelling of the bony cortices (Björk, 1963; Rune, 1980). It was therefore essential to establish the stability of the implants before they could be used as valid reference markers.

The validation of implant stability was carried out by measuring the distances between the implants on each radiograph (at 1:1 magnification) and then comparing the distances between the pairs of serial radiographs. The implants forming each implant pair were only accepted as stable where the inter-implant distances differed between the radiographs by less than 0.64 mm; otherwise, the implant pair was rejected. This value represents the 99.9 per cent confidence limit for the differences in inter-implant distance arising from random error (Table 1).

Identification of potentially stable sites

The images of each pair of radiographs were superimposed and registered on the stable implants, thereby establishing a common co-ordinate system for the two radiographs. Corresponding regions approximately 1 cm square were then carefully compared sequentially across the entire mandibular image, avoiding the crowns and roots of the teeth.

Image cross-correlation

When potentially stable structural details were found, the full extent of the perimeter of the structure was located and its co-ordinates (relative to the implants) were recorded. An area of the image around the structure on the earlier radiograph was then selected and used as a 'template'. A search was then conducted across a much larger region from the later radiograph (the 'search area') to locate the precise position of any site matching the structure within the template. The search area was at least four times the area of the template with the centre of the search area located at the same co-ordinates as the template (Figure 1).

The search and match procedure was carried out automatically by computer using the mathematical procedure known as cross-correlation (Pratt, 2007). In effect, the template is shifted pixel by pixel both vertically and horizontally across the search area; at each shifted position, the correlation is calculated between the template and that part of the search area over which it lies. This

Table 1 Method errors.

		Systematic error (mm)			Random error (mm)	
	N	Mean difference	*t*-test	*P*	SD	99.9% confidence limit
Inter-implant distance	102	−0.02	0.63	0.53 NS	0.19	0.64
Location of cross-correlation peak	34	0.21*	—	—	0.18**	0.59

NS, indicates not statistically significant ($P > 0.05$).
*It was not possible to test for a systematic error between the two determinations of the cross-correlation peak because the differences were measured as absolute distances.
**Calculated from the relationship between the mean absolute difference and the standard deviation (SD) of the underlying distribution (with zero mean) (Bland and Altman, 1999).

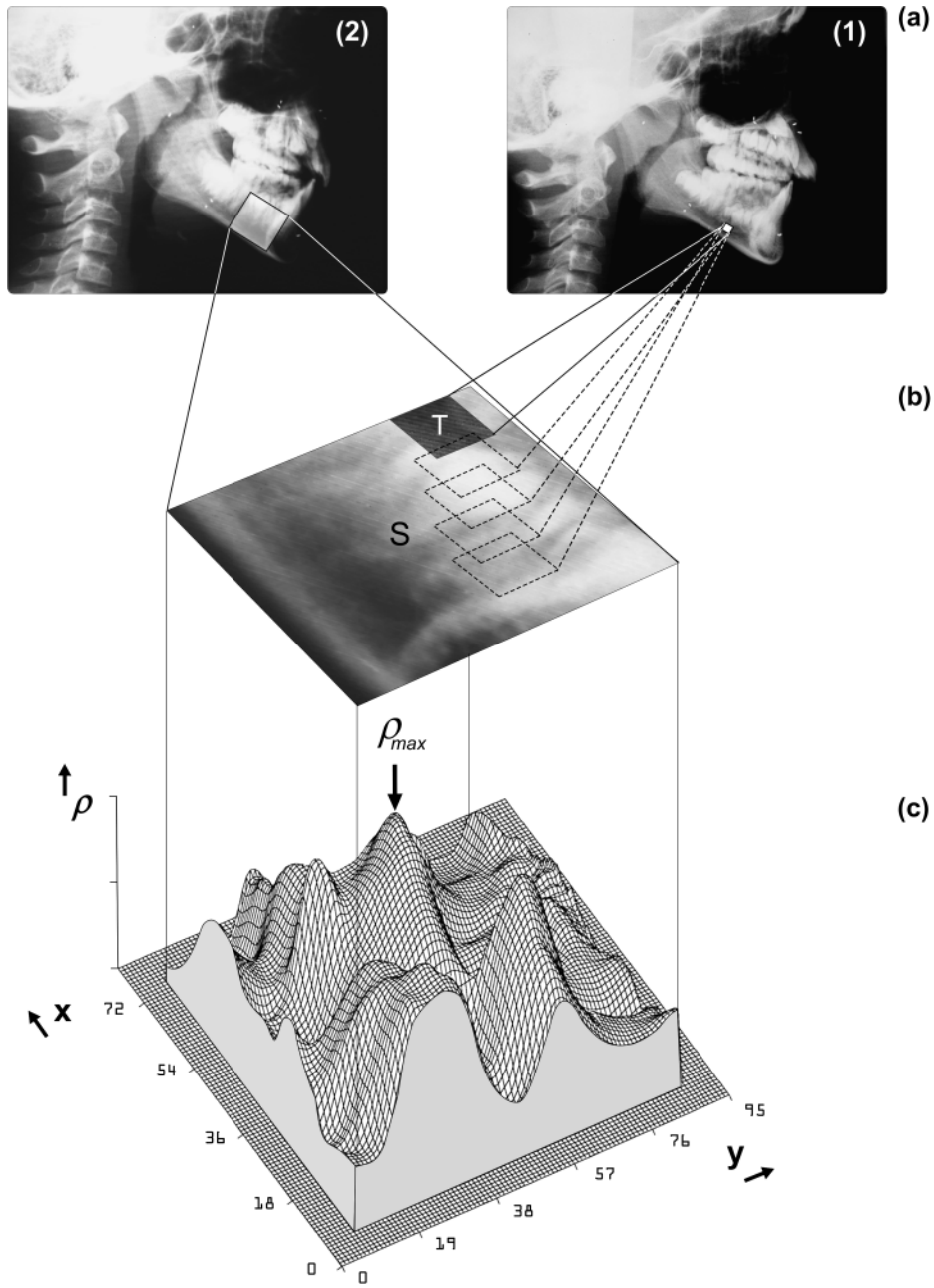

Figure 1 Diagrammatic representation of the cross-correlation procedure: (**a**) initial (1) and later (2) radiographs; (**b**) the 'template' from the earlier radiograph is shifted pixel by pixel across the 'search area' from the later radiograph. At each shifted position, the cross-correlation is calculated between the template and that part of the search area over which the template lies. (**c**) Cross-correlation map showing the point of maximum probability of match (ρ_{max}).

procedure produces a three-dimensional mathematical function of the spatial distribution of the correlation over the entire search area (Figure 1c).

If the structure for which validation is being sought is indeed stable, the maximum value of the cross-correlation function should occur when the template and that part of the search area over which it is aligned are at identical spatial positions relative to the implants in the two radiographs. This would then confirm that the anatomical structure was both present and in an identical location (relative to the implants) on both radiographs and thus could be deemed to represent a stable anatomical structure.

In practice, the measurement of the spatial position of the peak will be subject to error. It was necessary therefore to set an upper bound on this error for the peak to be accepted as a true match. This was achieved by reference to the random error for the location of the cross-correlation peak. Only where the measured peak occurred within 0.59 mm of the implant determined position was it accepted as indicating a true match. This value represents the upper bound of 99.9 per

cent confidence interval for the differences in position of the cross-correlation peak arising from random error (Table 1).

The basic manipulation and measurements of the digital images were made using Image Tool version 3 (University of Texas Health Sciences Center, San Antonio, Texas, USA) and the detection of potentially stable structures was carried out using the variable transparency feature of CorelXara® imaging software (Corel Corporation, Ottawa, Ontario, Canada). The cross-correlations were calculated and mapped using the least squares cross-correlation program, CORR (Wiles and Foreshaw, 1993).

Statistical methods and error of the method

The magnitude and direction of the relationship between the numbers of NRS found in each subject and (1) the age at the initial radiographs and (2) the interval between the radiographs was assessed by correlation. Spearman's rank correlation coefficient (r_{rank}) was employed rather than the more usual Pearson product–moment coefficient because, in both cases, the joint distribution of the variables was non-linear.

The random error of measurement for the inter-implant distances was calculated from replicate measurements of the inter-implant distance for each implant pair made under similar conditions several weeks apart. The replicate measurements were then combined to form double-determination pairs and the random error was calculated as described by Jaech (1985). The possibility of systematic error between the double determinations was examined using a one-sample Student's *t*-test.

The random error for the location of the cross-correlation peak was determined by repeating the process of locating and cross-correlating the template and search areas for one arbitrarily selected candidate site from the earlier radiograph of each pair for all 34 subjects. The random error was calculated from the absolute differences in positions of the peak between the repeat and original location found in the main study using the method described by Bland and Altman (1999). The possibility of systematic error between the double determinations of the cross-correlation peak could not be examined because absolute (rather than signed) differences were used. The method errors are shown in Table 1.

Results

Visual comparison of the superimposed images followed by validation using cross-correlation revealed structural details that remained stable (NRS) across the serial radiographs of each subject. The smallest number of NRS was four (2 subjects), the largest was 15 (3 subjects), and the median was nine. The number of distinct stable structures was positively correlated with age at the initial radiograph (r_{rank} = 0.385, P = 0.024) but showed no significant association with the time interval between the radiographs (r_{rank} = −0.211, P = 0.234).

The NRS were not evenly distributed across the mandibular image but tended to cluster near the inferior border and were most numerous in the anterior half of the mandible and particularly in the mental interforaminal region. They were fewest in the ascending ramus and none were found above the level of the mandibular foramen (Figure 2).

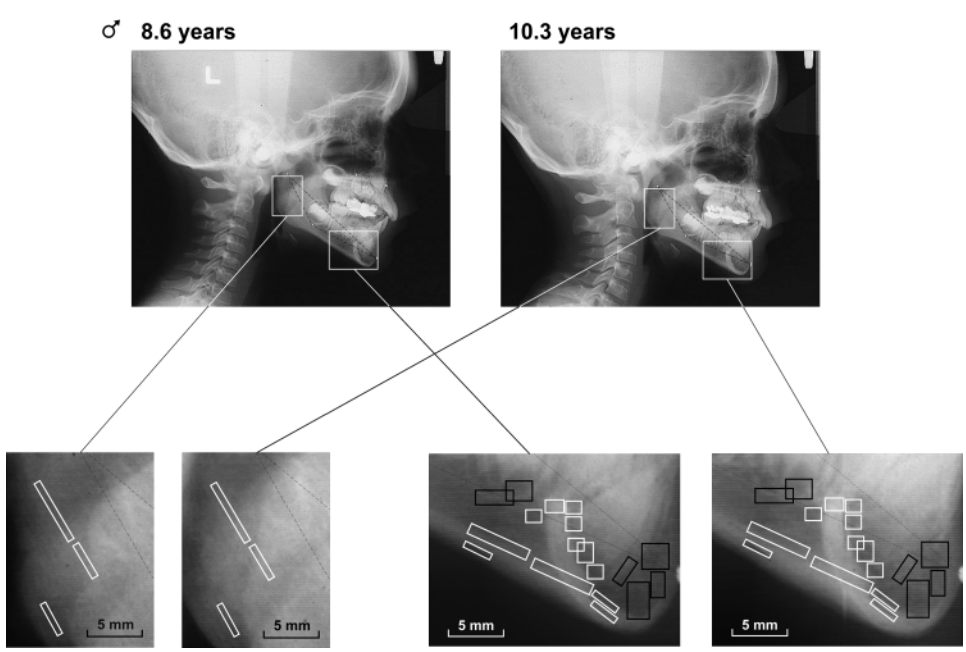

Figure 2 An example of the serial radiographs used in the study. In the lower illustrations, the regions enclosed in white boxes contain (stable) structures that correspond on earlier and later images; the regions enclosed in black boxes appear to correspond in the two images but are not stable because remodelling or 'drifting' has occurred between the recording of the radiographs.

Two situations of interest arose during the process of validating potentially stable structures (candidate sites) in the most anterior region of the mandible. First, several candidate sites detected within the symphysis were rejected as unstable when examined by cross-correlation because of relocation or drift of the radiopaque outline of these structures—presumably due to gradual remodelling (the structures in black boxes in Figure 2). Second, narrow regions of the external contour of the symphysis (bony chin) often remained in the same location but it was not possible to validate the stability of these regions because they lacked sufficient identifying detail. In addition, the part of the chin that appeared to remain stable varied from subject to subject. In some cases, it was high up at the point of inflexion of the external contour and in others it occurred at the most prominent point of the chin or, occasionally, substantially more inferiorly.

Anatomical designation of the structures

On the basis of their morphology, the NRS could be grouped into two distinct classes: a small group consisting of amorphous condensations in the bone and prominent (radiodense) trabeculae and a larger group consisting of (usually paired) lines of bony compacta. Within this latter group, the spatial patterning of the distribution of the structures and the consistent patterns identified point strongly to well-defined anatomical entities being responsible for the radiographic appearance rather than simply arbitrary thickening of the bony trabeculae.

Nine primary structures were identified, as shown in Figure 3. The anatomical designation of these structures was determined by reference to a range of anatomical and radiographic sources but primarily the classic descriptive studies by Hirschfeld (1923), Ennis (1937), Shiller and Wiswell (1954), Benkow (1961), Carter and Keen (1971), and Sutton (1974) together with more modern studies by Anderson *et al.* (1991), Gahleitner *et al.* (2001), and Mraiwa *et al.* (2003).

It is important to realize, however, that there are limits to the anatomical inferences that can be drawn from single perspective films and that both the anatomy and radiographic interpretation of the internal structures of the mandible are still controversial areas, particularly in the mental interforaminal region (Baldissera and Silveira, 2002; Trikeriotis *et al.*, 2008). Consequently, the designations should not be seen as definitive or final but rather as tentative and subject to revision.

In this context, a particular problem arose with the anatomical designation of the two NRS in the form of paired (possibly bilateral) linear bands passing anteriorly into the symphysis from above and below the approximate region of the mental foramen. It seems likely that these linear bands represent the corticated walls of the neurovascular canals arising from the superior and inferior genial spinal foramina (Baldissera and Silveira, 2002; Mraiwa *et al.*, 2003). In the majority of cases, however, this was probably not the correct designation because the bands extended posteriorly beyond the lingual symphyseal margin. As a consequence, the exact anatomical nature of these bands remains uncertain and, at present, it may be more sensible to avoid specific but potentially incorrect anatomical designations and simply employ the general terms ‘superior’ and ‘inferior interforaminal striae’.

Discussion

Limitations of the study

Before discussing the results of this study, it is important to recognize that no structure within a living subject can be totally stable, at least at the ultrastructural or cellular levels. The concept of stability is useful, however, at the microstructural and macroscopic levels where we wish to make quantitative measurements of clinically meaningful changes. At these spatial scales, we are concerned to establish limits on the level of instability of the reference structures. That is, the best we can ask for is that the level of instability of the reference structures should be too small to have any detectable influence on the measurements. From a practical perspective, if the level of instability of a reference structure is smaller than the spatial resolution of the radiographic system, then this cannot be distinguished from genuine stability. In the case of conventional cephalometric radiographs recorded with a screen–film system, total movement or instability of less than approximately 0.2 mm (over whatever maximum time period is to be considered) will be undetectable (Barrett and Swindell, 1981; Ishizuka, 1981) and is indistinguishable from ‘true’ stability.

The nature of the reference structures

The purpose of this study was to locate stable structures within the mandibular image that could be used as valid reference markers. Although the brightness and contrast were equalized for each pair of films, no other processing or visual enhancement of the images was performed prior to the detection stage. Nevertheless, the detection of stable structures was not difficult. The finding that there are many previously unreported NRS and that they are widely distributed throughout the mandible is, at first, a little surprising given the number of cephalometric studies which have been conducted on subjects with tantalum markers over the last 50 years. This raises the question that if these structures are so numerous and easily visible why have they eluded detection for so long? The answer probably lies in the difficulty of directly superimposing and analysing serial radiographs. The NRS found in this study required the examination of small details in the radiographic images. Such details are not easily amenable to tracing and have thereby probably eluded detection because it has generally been the tracings and not the original films that were superimposed and compared as in the case of Julius (1972).

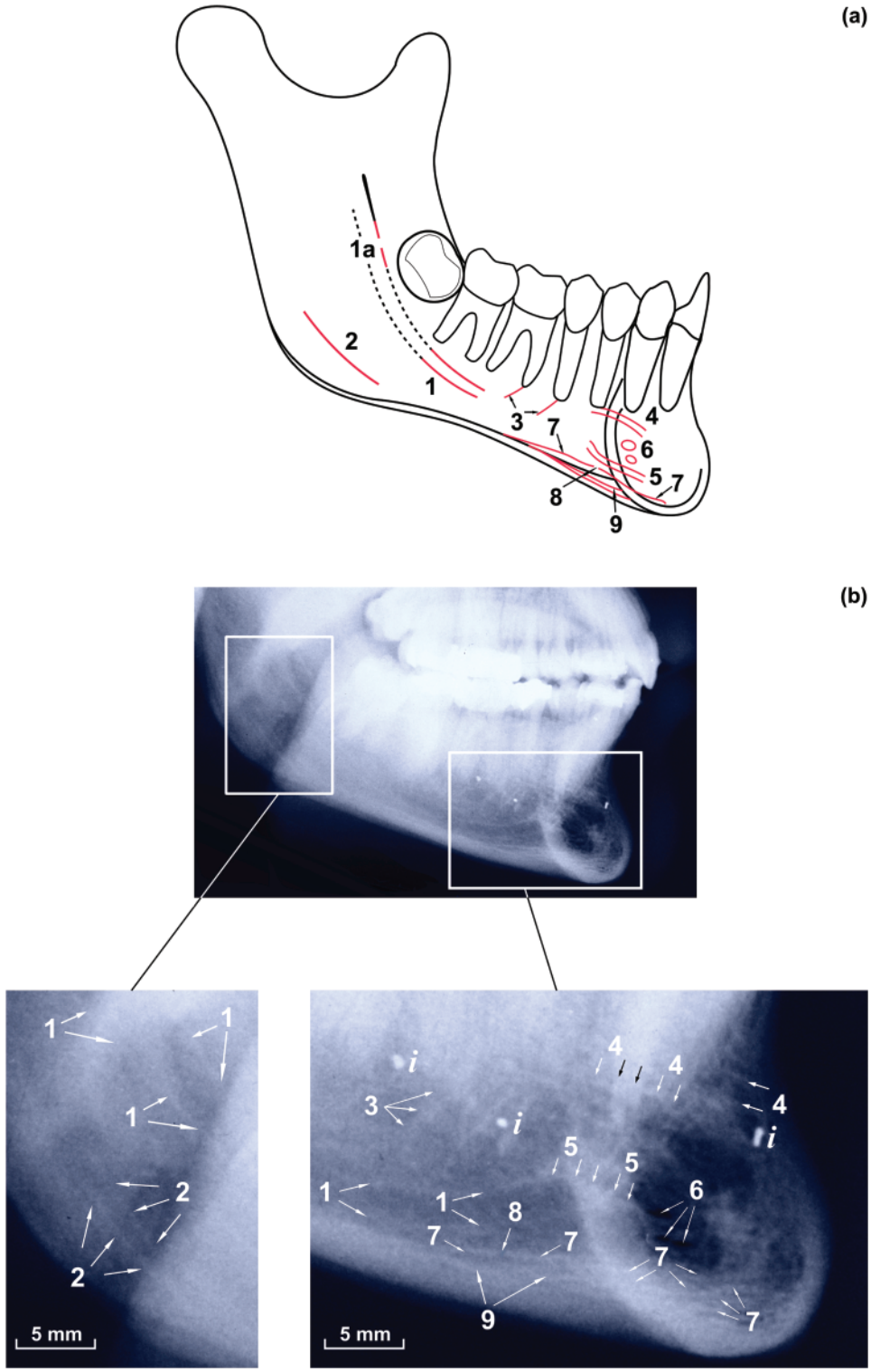

Figure 3 Natural reference structures (NRS) detected and validated in the study. (**a**) Diagrammatic representation of the general form and location of the NRS; (**b**) examples of the NRS seen on the cephalometric radiograph of a subject from the study. Key to the NRS: (1) Corticated margins of the mandibular canal (in children older than ~9 years); (1a) Sections of the superior margin of the mandibular canal distal to the second permanent molar; (2) Accessory supra-gonial (inferior ramal) neurovascular canal; (3) Apical neurovascular (nutrient) canals; (4) Superior interforaminal striae; (5) Inferior interforaminal striae; (6) Intra-symphyseal transverse neural canals; (7) Juxtacortical endosteal lamellae; (8) Lateral lingual (retromental) canal; (9) Intra-cortical striae. The tantalum implant markers appear as radiopaque dots and are indicated by the letter '*i*'.

However, some investigators have previously called attention to the constant relationship between the more prominent trabeculae in the jaws and implant markers. For example, Poulton (1968) and Björk and Skieller (1983) suggested that any 'prominent trabecular feature' within the symphysis could be used as a reference structure. This later suggestion is not wholly supported by the findings of the present study. That is, although many of the more prominent features in the symphyseal image appeared on both radiographs, the majority appeared to move relative to their original, implant-defined positions. This was presumably due to gradual remodelling, which makes them unreliable as growth markers. An analogous situation has been seen in some of the NRS used for evaluation of growth in the long bones of the arm and leg where resorption acts unequally on the margins of transverse lines ('Harris lines') leading to gradual drift of these reference structures (Garn *et al.*, 1968).

Only those structures that delineate the boundaries of the most prominent neurovascular canals that enter and leave, or are contained within, the symphyseal region were both persistent and immobile relative to the implant markers.

This finding was, however, not carried over to the main neurovascular canal in the body of the mandible—the mandibular canal—which, in the youngest subjects, was not found to be morphologically or spatially stable. This is an interesting but not unexpected finding and was not simply related to difficulties in locating or visualizing the margins of the mandibular canal. It seems likely that in the youngest subjects, the mandibular canal would not have completed its developmental migration beneath the molars and developing premolars where it gradually fuses with a smaller inferolateral canal, 'Serres' canal' (Tsusaki, 1950; Wendler *et al.*, 1980).

In those subjects at the later stages of development, where the bony margins of the mandibular canal were clearly visible throughout the body of the mandible, the canal remained both morphologically and spatially stable. This finding supports the earlier reports by Björk (1963) and Julius (1972).

Although it was not the purpose of this study to examine the validity of Björk's structures, it is interesting to note that of the three remaining structures mentioned by Björk (1963, 1969) and Björk and Skieller (1983), the internal inferior contour of the symphysis, the anterior contour of the bony chin, and the lower (bony) contour of the third molar germ before root development begins, none were identified as stable structures. In the case of the third molar germ, there were too few subjects with third molars at the appropriate stage of development for any conclusion to be drawn. In the case of the bony chin, although variable parts of this contour were identified as potentially stable sites in some subjects, the region lacked sufficient morphological detail to allow it to be precisely and unambiguously located on both radiographs. Consequently, it is not possible to judge from the present study whether or not it was stable.

Even in the absence of fine morphological detail, however, it was clear that the internal inferior contour of the symphysis was generally unstable. Occasionally, marked differences were observed in the position of this contour, indicating that it is far from stable in some subjects, as seen in Figure 4. Instability of the inner inferior contour of the symphysis has been previously reported by several researchers, including Björk (1963) who indicated that the contour could be unstable (as could the anterior contour of the chin) in cases of severe backward growth rotation.

While it has long been suspected that some neurovascular and nutrient canals might be stable (Payton, 1932; Moss *et al.*, 1959), the lamella structure of the mandibular cortex

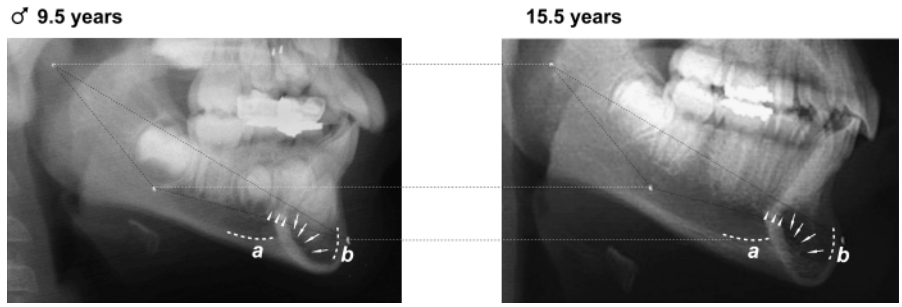

Figure 4 Serial cephalometric radiographs showing the sites that can be used for rapid and accurate superimposition (the 'simplified method' described in the text). The dotted outlines indicate (**a**) the inner (endocortical) surface of the inferior cortex below the canine and premolars and (**b**) the inner anterior surface of the symphysis (the internal surface of the bony chin). These two sites alone should provide a reasonably accurate superimposition in most cases where the interval between radiographs is short (<2.5 years). Where the interval is greater or where fine-tuning is required, the images can be adjusted to align the structures indicated by white arrows. The white arrows point to the transverse neurovascular canals in the posterior inferior third of the symphysis. The white arrowheads without stems indicate the superior interforaminal striae as they cross the posterior outline of the symphysis. Note the marked resorption and remodelling of the inner inferior contour of the symphysis between earlier and later radiographs making this site unsuitable as a reference structure.

has not previously attracted any attention as a source of stable structures. It seems likely that little attention has been directed to this region of the mandible because it has long been viewed as being continuously remodelled during growth. This remodelling is largely appositional and, in the age range examined in this research, it appears to leave the inner (endocortical) surface largely intact. Where, however, the cortex is subject to extensive remodelling (beneath the ascending ramus and angle), no cortical NRS were found.

Although it appears that these cortical NRS are incremental 'tree-ring'–like structures within the cortex, it seems much more likely that they are approximately linear bands lying at or just superior to the endocortical margin, the lateral cephalometric projection being responsible for the apparent inclusion of the lamellae within the cortex. More detailed radiographic examination using different projections will be required to resolve this issue.

In all cases where these structures were evident on both radiographs (within or close to the inferior cortex and just distal to the symphyseal shadow), they were both persistent and immobile in relation to the stable implant markers.

Clinical application

The size and nature of the fine details delineating the NRS found in this study means that few of these structures will be amenable to tracing. Consequently, this implies that direct superimposition of the radiographs will be required to make use of them. With the increasingly widespread use of digital imagery in clinical practice, this should, perhaps, pose less of a problem now than in the past.

However, one major difficulty in applying the findings of the present study to the superimposition of clinical radiographs is distinguishing the right and left sides of the mandibular body and ascending ramus. In clinical practice, there are always unavoidable differences in the projection from film to film which lead to differences in the superimposition of the two sides of the mandible. Consequently, structures close to the midline should be preferred to overtly bilateral structures in the posterior of the mandibular body or ascending ramus.

With this in mind, the mandibular images should first be grossly aligned vertically using the endocortical margin and juxtacortical lamellae of the inferior cortex beneath the canine and first premolar (structure 7, Figure 3) and then brought into fine horizontal alignment using the transverse neurovascular canals in the posterior inferior third of the symphysis (structure 6, Figure 3). This should produce an accurate vertical and horizontal superimposition in the anterior midline. A final rotational adjustment may then be required to bring the mandibular and supra-gonial canals on earlier and later images into alignment (structures 1, 1a, and 2, Figure 3). If two separate posterior orientations are required to align the mandibular and supra-gonial canals, then, for the clinical situation, these should be averaged to produce a single (posterior) orientation between the earlier and later images.

Alternatively, a simplified method that should provide a rapid but accurate superimposition in the majority of cases would be to align the mandibular images using (1) the inner (endocortical) surface of the inferior cortex below the canine and premolars and (2) the inner anterior surface of the symphysis (the internal surface of the bony chin). While recognizing that both contours are subject to gradual remodelling, the magnitude of the change is very small during all periods examined in this study. If fine-tuning of the superimposition is required, it can be achieved by adjusting the images to bring the transverse neurovascular canals and the superior interforaminal striae into alignment. In younger subjects, the latter structure is most easily seen where it crosses the posterior symphyseal border (Figure 4).

Although the validity of these methods is derived from, and supported by, the findings of this study, they have not been tested in an independent implant sample nor has their precision been examined in clinical practice.

Finally, it is worth noting that there are some structures that appear remarkably stable but which remodel and undergo continuous relocation during growth, presumably due to gradual remodelling of the bone. Where stable implanted markers are available, there is no real danger of wrongly identifying them as 'stable', but in clinical cases and in cephalometric research, without the aid of tantalum implants, such mistakes will be easy to make. In this regard, particular care should be taken to avoid using the mandibular canal close to the mandibular foramen and lingula; prominent trabecular patterns seen within the anterior half of the symphysis; and the internal inferior contour of the symphysis (as noted above).

Conclusions

The experimental method has proved to be effective in detecting and validating several hitherto unknown NRS on the lateral cephalometric image of the mandible. It has also cast doubt on the stability of two structures previously reported to be stable (the inner inferior contour of the symphysis and prominent trabeculae within the symphysis).

Some of the NRS found in this study may prove difficult to identify on routine clinical radiographs but those structures at, or close to, the endocortical margins should be relatively easy to locate and apply in cephalometric analysis of patients and in clinical research studies.

Address for correspondence

S. D. Springate
111 Harley Street
London W1G 6AW
UK
E-mail: orthodontics@london.com

Acknowledgements

I wish to express my sincere gratitude to the late Dr J. Rodney Mathews of the University of California at San Francisco, to Professor Sheldon Baumrind of the University of the Pacific, and to Professor Robert Little of the University of Washington for allowing access to the material that formed the basis of this study. I am also very grateful to Dr Mike Foreshaw of the Department of Physics and Astronomy, University College London for allowing me to use and adapt the cross-correlation program, CORR. Finally, I warmly thank Steve Jones for his helpful advice and suggestions on the preparation of the manuscript.

References

Anderson L C, Kosinski T F, Mentag P J 1991 A review of the intraosseous course of the nerves of the mandible. Journal of Oral Implantology 17: 394–403

Baldissera E Z, Silveira H D 2002 Radiographic evaluation of the relationship between the projection of genial tubercles and the lingual foramen. Dentomaxillofacial Radiology 31: 368–372

Barrett H H, Swindell W 1981 Radiological imaging. Vol. 1: Academic Press, New York

Benkow H H 1961 Roentgenological and morphological findings in the region of the mandibular symphysis. Acta Odontologica Scandinavica 19: 1–21

Björk A 1955 Facial growth in man, studied with the aid of metallic implants. Acta Odontologica Scandinavica 13: 9–34

Björk A 1963 Variations in the growth pattern of the human mandible: longitudinal radiographic study by the implant method. Journal of Dental Research 42: 400–411

Björk A 1968 The use of metallic implants in the study of facial growth in children: method and application. American Journal of Physical Anthropology 29: 243–254

Björk A 1969 Prediction of mandibular growth rotation. American Journal of Orthodontics 55: 585–599

Björk A, Skieller V 1983 Normal and abnormal growth of the mandible: a synthesis of longitudinal cephalometric studies over a period of 25 years. European Journal of Orthodontics 5: 1–46

Bland J M, Altman D G 1999 Measuring agreement in method comparison studies. Statistical Methods in Medical Research 8: 135–160

Brodie A G 1949 Cephalometric roentgenology, history, technics and uses. Journal of Oral Surgery 7: 185–198

Carter R B, Keen E N 1971 The intramandibular course of the inferior alveolar nerve. Journal of Anatomy 108: 433–440

Cook P A, Gravely J F 1988 Tracing error with Björk's mandibular structures. Angle Orthodontist 58: 169–178

Ennis L M 1937 Roentgenographic variations of the maxillary sinus and the nutrient canals of the maxilla and mandible. International Journal of Orthodontia and Oral Surgery 23: 173–193

Feasby W H 1981 A radiographic study of dental eruption. American Journal of Orthodontics 80: 554–560

Gahleitner A, Hofschneider U, Tepper G, Pretterklieber M, Schick S, Zauza K 2001 Lingual vascular canals of the mandible: Evaluation with dental CT. Radiology 220: 186–189

Garn S M, Silverman F N, Hertzog K P, Rohmann C G 1968 Lines and bands of increased density. Medical Radiography and Photography 44: 58–89

Hirschfeld I 1923 A study of skulls in the American museum of natural history in relation to periodontal disease. Journal of Dental Research 5: 241–265

Isaacson R J 1996 Superimposition and structural analysis. American Journal of Orthodontics and Dentofacial Orthopedics 109: 193–195

Isaacson R J, Erdman A G, Hulgren B W 1981 Facial and dental effects of mandibular rotation. In: Carlson D S, Ribbens K A (eds). Craniofacial biology. Monograph 10, Craniofacial Growth Series. Center for Human Growth and Development, University of Michigan, Ann Arbor. pp. 146–156

Ishizuka R 1981 The quantitative analysis of the mandibular trabecular X-ray image through two dimensional Fourier transform. Nihon University Journal of Oral Science 7: 149–159

Jaech J L 1985 Statistical analysis of measurement errors. John Wiley and Sons, New York

Julius R B 1972 A serial cephalometric study of the metallic implant technique and methods of maxillary and mandibular superimposition. Thesis, University of Washington

Mathews J R, Payne G S 1980 Quantitative computerized analysis of lower incisor changes: a longitudinal implant study in man. Angle Orthodontist 50: 218–229

Moss M L, Greenberg S N, Noback C R 1959 Developmental migration of mandibular buccal dentition in man. Angle Orthodontist 29: 169–176

Mraiwa N, Jacobs R, Moerman P, Lambrichts I, van Steenberghe D, Quirynen M 2003 Presence and course of the incisive canal in the human mandibular interforaminal region: two-dimensional imaging versus anatomical observations. Surgical Radiology and Anatomy 25: 416–423

Payton C G 1932 The position of the nutrient foramen and direction of the nutrient canal in the long bones of the madder-fed pig. Journal of Anatomy 68: 500–510

Poulton D R 1968 Evaluation of space-closing techniques with the aid of laminagraphic cephalometrics. American Journal of Orthodontics 54: 899–919

Pratt W K 2007 Digital image processing. John Wiley and Sons, New York

Rune B 1980 Roentgen stereophotogrammetry and metallic implants in the study of craniofacial anomalies. Thesis, University of Lund, Malmö

Shiller W R, Wiswell O B 1954 Lingual foramina of the mandible. Anatomical Record 119: 387–390

Springate S D, Jones A G 1998 The validity of two methods of mandibular superimposition: a comparison with tantalum implants. American Journal of Orthodontics and Dentofacial Orthopedics 113: 263–270

Sutton R N 1974 Anatomical variation in the region of the mandible. Dentomaxillofacial Radiology 3: 77–89

Trikeriotis D, Paravalou E, Diamantopoulos P, Nikolaou D 2008 Anterior mandible canal communications: a potential portal of entry for tumour spread. Dentomaxillofacial Radiology 37: 125–129

Tsusaki T 1950 On a new finding of the development of the mandibular canal. Yokohama Medical Bulletin 1: 27–33

Wendler D, Bertolini R, Röhner O 1980 Die embryofetale Entwicklung des Canalis mandibulae beim Menschen. In: Schumacher G H, Fanghänel J, Lange H (eds). Oral-Anatomie Eigen-Verlag Universität Rostock, Rostock, pp. 46–51

Wiles C, Foreshaw M R 1993 Recognition of volcanoes on Venus using correlation methods. Image and Vision Computing 11: 188–196